

Cubature Kalman Filter-based Performance Enhancement of Wireless Indoor Localization using Ultra-wideband

Seong Yun Cho

School of Robotics Engineering, Kyungil University, 50 Gamasilgil, Hayangup, Kyungsan, Republic of Korea

Keywords: Indoor Wireless Localization, Ultra-wideband, Cubature Kalman Filter.

Abstract: Ultra-wideband has been widely used for accurate wireless indoor localization systems due to accurate ranging measurement capability. There are several methods for ranging-based localization systems: iterative methods, linear closed-form solutions, model-based filters, etc. These methods have their advantages and disadvantages. In this paper, the characteristics of these methods are analysed and a cubature Kalman filter-based localization method is presented to improve the localization performance in various indoor environments.

1 INTRODUCTION

In the indoor space, location information is used as key information for robot control and distribution control as well as various location-based services. The location estimation technique can be divided into a sensor based and a communication based, and the communication based localization is performed using distance data, angle data, and signal strength data obtained through communication. In this paper, distance measurement based localization techniques are discussed (Kolodziej and Hjelm, 2006; Banani et al., 2013; Silva and Hancke, 2016).

In order to measure the distance based on communication, time-of-arrival (ToA) technique is used when the nodes are synchronized with each other, and two-way-ranging (TWR) technique is used when the time synchronization is not achieved. Recently, accurate localization systems have been developed by using Ultra-Wideband (UWB) which can measure accurate distance easily by TWR technique. The UWB can acquire distance measurements with a resolution of 30cm or less by using microwave having a bandwidth of 500Mhz or more (Oh et al., 2009; Cho, 2014). In addition, the UWB signal has a higher obstacle transparency, which is higher than other signals in the indoor space. However, additional distance measurement errors due to multipath signals can not be avoided in indoor space (Lee and Scholtz, 2002; Lee et al., 2013; Yan et al., 2013; Cho, 2014; Silva and Hancke,

2016). In this environment, various localization algorithms show different performance.

In this paper, various localization methods are summarized; iterative least squares (ILS) method, direct solution (DS) method, and difference of squared ranging measurements (DSRM) method. The advantages and disadvantages of each method are analyzed and a cubature Kalman filter (CKF)-based localization filter is designed to avoid the disadvantages. The CKF-based localization filter enables state variable expansion to estimate the channel-specific error and is left as a future study. After analyzing the properties of the methods in equation expansion, it is shown that the performance of the CKF-based localization method is superior to other methods in indoor environment through simulation results.

2 WIRELESS LOCALIZATION METHODS

For wireless localization, the following ranging measurement equation is most basic (Cho et al., 2017).

$$\tilde{r}_i = \sqrt{(x_i - x_M)^2 + (y_i - y_M)^2} + b_i + w_i \quad (1)$$

where \tilde{r}_i is the ranging measurement between an anchor node (AN) i and a mobile node (MN), $[x_i \ y_i]^T$ and $[x_M \ y_M]^T$ are the locations of the AN

i and MN, respectively, b_i is the non-Gaussian error, and w_i is the white Gaussian noise.

Various methods for estimating the location of MN based on this equation have been studied (Mendel, 1995; Biton et al., 1998; Arasaratnam and Haykin, 2009; Cho and Kim, 2013). In this section, the advantages and disadvantages of these methods are analysed and finally a location estimation filter based on the CKF is designed.

2.1 Iterative Least Squares

To linearize the nonlinear equation (1), in the ILS method, the first order Taylor series expansion of equation (1) is performed using the nominal point that is initially set. The linearized equation can be yield as following matrix form.

$$R = HX + W \tag{2}$$

where

$$X = [\delta x_M \quad \delta y_M]^T \tag{3a}$$

$$R = [\tilde{r}_1 - \bar{r}_1 \quad \dots \quad \tilde{r}_n - \bar{r}_n]^T \tag{3b}$$

$$H = \begin{bmatrix} (\bar{x}_M - x_1) / \bar{r}_1 & (\bar{y}_M - y_1) / \bar{r}_1 \\ \vdots & \vdots \\ (\bar{x}_M - x_n) / \bar{r}_n & (\bar{y}_M - y_n) / \bar{r}_n \end{bmatrix} \tag{3c}$$

$$W = \begin{bmatrix} b_1 + w_1 \\ \vdots \\ b_n + w_n \end{bmatrix} \tag{3d}$$

In this equation, n is the number of the ANs, $[\bar{x}_M \quad \bar{y}_M]^T$ is the nominal point, and \bar{r}_i is the calculated range using the nominal point as $\sqrt{(x_i - \bar{x}_M)^2 + (y_i - \bar{y}_M)^2}$. The nominal point error can be estimated as follows (Mendel, 1995):

$$\hat{X} = (H^T H)^{-1} H^T R \tag{4}$$

The location of the MN can be updated as

$$\begin{bmatrix} \hat{x}_M \\ \hat{y}_M \end{bmatrix}_{ILS} = \begin{bmatrix} \bar{x}_M \\ \bar{y}_M \end{bmatrix} + \hat{X} \tag{5}$$

This process is iterated until $\hat{X}^T \hat{X}$ is smaller than the threshold that is set previously. In this process, two main issues have to be considered: the large initial error of the nominal point may cause local minimum problem; the non-Gaussian error as well as the Gaussian noise cannot be taken into account. The former problem can be solved using the

particular algorithm. However, it is difficult to overcome the latter problem and this causes unavoidable localization errors.

2.2 Direct Solution

In the DS method, the measurement errors in the equation (1) are ignored, then the both sides of (1) are squared to remove the square root. The DS method yields a closed-form solution as follows (Biton et al., 1998):

$$\begin{bmatrix} \hat{x}_M^i \\ \hat{y}_M^i \end{bmatrix}_{DS} = -L \left(A + B \frac{-b + (-1)^i \sqrt{b^2 - 4ac}}{2a} \right) \tag{6}$$

where $i \in \{1, 2\}$,

$$L = (G^T G)^{-1} G^T \tag{7a}$$

$$G = \begin{bmatrix} 2x_1 & 2y_1 \\ \vdots & \vdots \\ 2x_n & 2y_n \end{bmatrix} \tag{7b}$$

$$A = \begin{bmatrix} \tilde{r}_1^2 - x_1^2 - y_1^2 \\ \vdots \\ \tilde{r}_n^2 - x_n^2 - y_n^2 \end{bmatrix} \tag{7c}$$

$$B = [-1 \quad \dots \quad -1]^T \tag{7d}$$

$$a = (LB)^T LB \tag{7e}$$

$$b = (2LA)^T LB - 1 \tag{7f}$$

$$c = (LA)^T LA \tag{7g}$$

The DS method has two candidate solutions, and one of them is selected based on the measurement residual calculated as

$$e(i) = \sum_{j=1}^n \left(\tilde{r}_j - \sqrt{(x_j - \hat{x}_M^i)^2 + (y_j - \hat{y}_M^i)^2} \right)^2 \tag{8}$$

The reduction of the computational burden is the merit of the DS method in comparison to the ILS method. There is the red sea zone (RSZ) problem, however, caused according to the relations among the locations of the ANs and MN (Cho and Kim, 2013). Also, the neglect of the measurement errors is the same as the ILS method.

2.3 Difference of Squared Ranging Measurements

The DSRM method, on the other hand, does not ignore the measurement errors. This method makes

the squared ranging measurements equations by squaring the both sides of the equation (1). One of the ANs is selected as a common node. Then, the DSRM equation is formulated by subtracting each squared ranging measurement equation of ANs from that of the common node as follows (Cho and Kim, 2013):

$$\begin{bmatrix} \rho_{1,C} \\ \vdots \\ \rho_{n-1,C} \end{bmatrix} = \begin{bmatrix} x_C - x_1 & y_C - y_1 \\ \vdots & \vdots \\ x_C - x_{n-1} & y_C - y_{n-1} \end{bmatrix} \begin{bmatrix} x_M \\ y_M \end{bmatrix} + V \quad (9)$$

$$\Leftrightarrow Z = G \begin{bmatrix} x_M \\ y_M \end{bmatrix} + V$$

where V contains the measurement errors.

The location of the MN can be calculated as

$$\begin{bmatrix} \hat{x}_M \\ \hat{y}_M \end{bmatrix}_{DSRM} = (G^T Q^{-1} G)^{-1} G^T Q^{-1} Z \quad (10)$$

where $Z = E[V \cdot V^T]$ can be calculated by assuming the non-Gaussian error is Gaussian noise.

The important thing in this method can be confirmed in the process of calculating $\rho_{j,C}$ as

$$\begin{aligned} \rho_{j,C} &= (\tilde{r}_j^2 - \tilde{r}_C^2 + \chi) / 2 \\ &= (r_j^2 - r_C^2 + \chi) / 2 + B + C + V \end{aligned} \quad (11)$$

where

$$\chi = x_C^2 + y_C^2 - x_j^2 - y_j^2 \quad (12a)$$

$$B = r_j b_j - r_C b_C + (b_j^2 - b_C^2) / 2 \quad (12b)$$

$$C = b_j w_j - b_C w_C \quad (12c)$$

$$V = r_j w_j - r_C w_C + (w_j^2 - w_C^2) / 2 \quad (12d)$$

The last three terms in this equation are related to the measurement errors, and there are several considerations: the size of the Gaussian noise is smaller than that of the non-Gaussian error; the non-Gaussian error is always positive numbers; and the last term V is considered in the equation (9) by Q . Based on the first consideration, it can be guessed that C is too small. Also B is analysed as a relatively small number due to the second consideration. Therefore, the DSRM method can yield more accurate solutions than ILS and DS methods even in the case of the measurement error that is not Gaussian.

2.4 Cubature Kalman Filter

The measurement equation the equation (1) is nonlinear. So, nonlinear Kalman filters such as extended Kalman filter, unscented Kalman filter (UKF), CKF, etc. can be used in the wireless localization. For the system model of the Kalman filter, a constant velocity (CV) model or constant acceleration model can be selected in the light of the dynamics of the MN. In this paper, the localization filter is designed using the CKF with a CV model.

CKF is the cubature rule-based approximate Bayesian filter, and the performance of the 3rd-degree CKF is similar to that of UKF (Arasaratnam and Haykin, 2009; Jia et al., 2013). If the CV model is defined in the 2-D coordinate frame, $2N$ cubature points ($\xi_i, i = 1, 2, \dots, 2N$, N is the system dimension, that is 4) are generated, and then time-propagated as follows:

$$\begin{aligned} \hat{\xi}_{i,k+1}^- &= \hat{\xi}_{i,k}^- (3) \cdot dt \\ \hat{\xi}_{i,k+1}^- &= \hat{\xi}_{i,k}^- (4) \cdot dt \\ \hat{\xi}_{i,k+1}^- &= \hat{\xi}_{i,k}^- (3) \\ \hat{\xi}_{i,k+1}^- &= \hat{\xi}_{i,k}^- (4) \end{aligned} \quad (13)$$

where dt is the time interval of the measurement acquisition, and the indices 1, 2, 3, and 4 denote location and velocity of x and y axes, respectively.

The time-propagated state vector and covariance matrix are calculated as follows:

$$\hat{x}_k^- = \sum_{i=1}^{2N} \frac{1}{2N} \hat{\xi}_{i,k}^- \quad (14)$$

$$P_k^- = \sum_{i=1}^{2N} \frac{1}{2N} (\hat{\xi}_{i,k}^- - \hat{x}_k^-) (\hat{\xi}_{i,k}^- - \hat{x}_k^-)^T + Q \quad (15)$$

where Q is the process noise covariance matrix.

Then, measurement-update of the state vector and error covariance matrix is performed as

$$\hat{x}_k = \hat{x}_k^- + K_k (\tilde{y}_k - \hat{z}_k^-) \quad (16)$$

$$P_k = P_k^- - K_k P_{xz}^T \quad (17)$$

where

$$\hat{z}_k^- = \sum_{i=1}^{2N} \frac{1}{2N} \hat{y}_{i,k}^- \quad (18a)$$

$$\hat{y}_{i,k}^- = [\hat{r}_{1,i,k}^- \ \dots \ \hat{r}_{n,i,k}^-]^T \quad (18b)$$

and the other parameters can be obtained in (Arasaratnam and Haykin, 2009).

New cubature points are generated as

$$\xi_{i,k} = S_k \sqrt{N} [1]_i + \hat{x}_k \quad (19)$$

where S_k can be calculated using the Cholesky factorization as $P_k = S_k S_k^T$.

The Kalman filter estimates the state variables using the systems equations as well as the measurements. That is, the model-based localization filtering can yield more accurate location solutions than the model-free localization methods when the model reflects the movement of the MN as it is. So, the solution of the Kalman filter can have good features of a low-pass filter. Also, the effect of the non-Gaussian measurement errors can be diminished.

3 SIMULATION ANALYSIS

To analyse the performance of the several model-free and model-based localization methods, some simulations are performed. In these simulations, it is assumed that the wireless communication infra used for localization is the UWB, so the noise of the ranging measurements is set to $N(0, (0.3m)^2)$. In addition, the non-Gaussian error denoted in (1) is defined as $|N(0, (1.5m)^2)|$. The size of the test area is set to $20\text{ m} \times 15\text{ m}$, and four ANs are installed in the area for the first simulation.

Figure 1 shows the comparative results of the localization methods. In this figure, four circles in the corners of the test area denote the ANs. Based on the error statistics, 1000 ranging measurements are generated each in the 24 fixed reference locations. The location of the MN is calculated using the individual localization method and, then, the location error is calculated. In this figure, the sized of the circles denote the comparative mean values of the location errors.

From the outcome of this simulation results, it can be stated that (i) the performance of the DS method may be degraded according to the test location due to the RSZ problem as can be seen in the top right of figure 1(b); (ii) among the model-free methods, the DSRM method has better localization performance than the DS and ILS methods because the non-Gaussian errors can be somewhat diminished in the DSRM method; and (iii) the location solution of the CKF is more accurate than the model-free methods because it uses the dynamic model of a MN as well as the ranging

measurement. The location errors at each test location are summarized in Table 1.

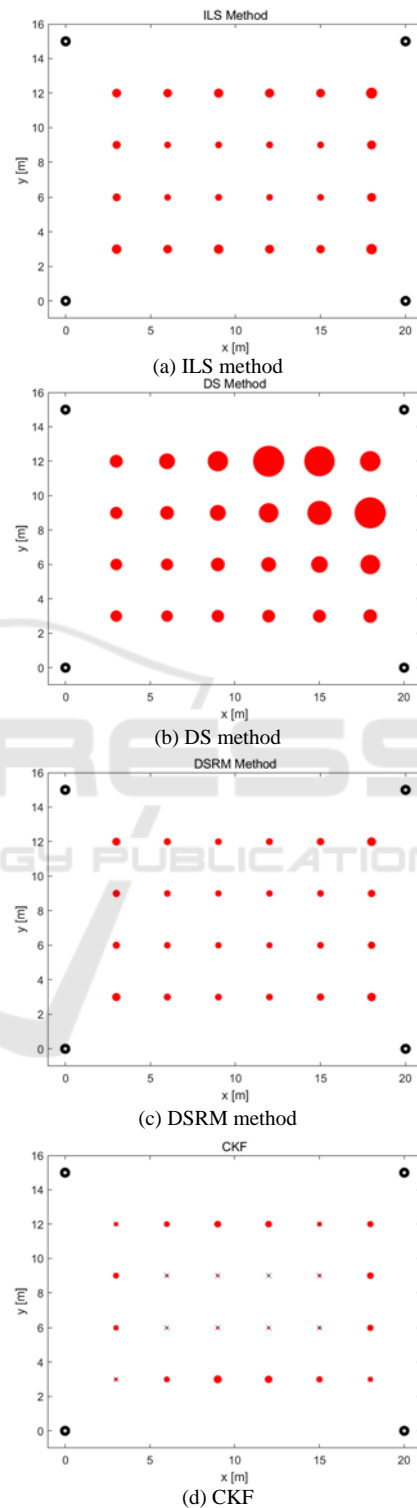
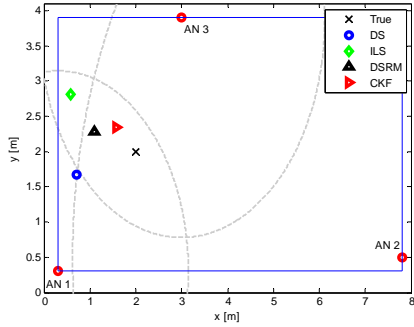


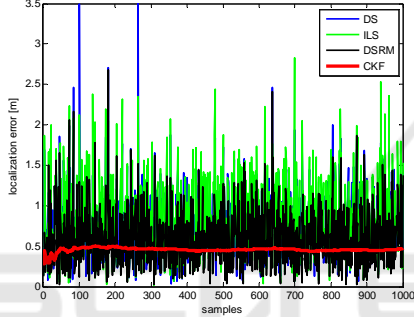
Figure 1: Simulation 1 – comparative localization errors according to the localization methods.

Table 1: Summary of Simulation 1 (1000 Samples).

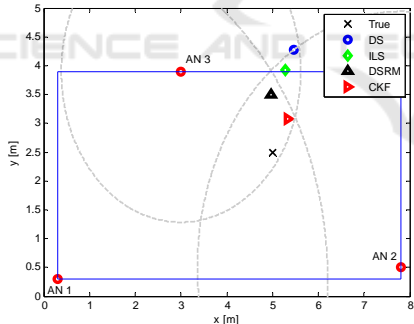
| Errors | Localization Methods | | | |
|----------|----------------------|-------|-------|-------|
| | DS | ILS | DSRM | CKF |
| Mean [m] | 2.559 | 1.248 | 1.071 | 0.723 |
| Std. [m] | 1.035 | 0.794 | 0.609 | 0.274 |



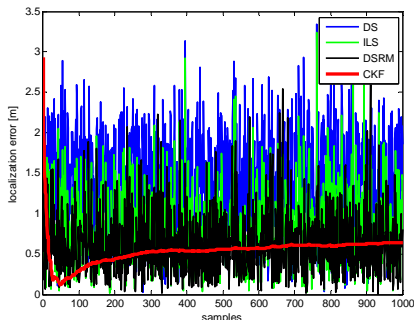
(a) an example of the localization (2 m, 2 m)



(b) localization errors (2 m, 2 m)



(c) an example of the localization (5 m, 2.5 m)



(d) localization errors (5 m, 2.5 m)

Figure 2: Simulation 2 – comparative results according to the localization methods in the small area.

Another simulation is performed and the results are shown in Figure 2. In this simulation, the small test area is set to $8\text{ m} \times 3\text{ m}$ and three ANs are installed in the test area denoted in Figure 2(a) and 2(c). Figure 2(a) and 2(b) are the results of the localization of the MN located in $(2\text{ m}, 2\text{ m})$, where the RSZ problem does not occur (Case 1). Figure 2(c) and 2(d) are the results of the localization of the MN located in $(5\text{ m}, 2.5\text{ m})$ where the RSZ problem occurs (Case 2).

In the Case 1, the results of the DS and ILS methods are similar, and that of the DSRM is improved. The CKF yields more accurate and stable solutions irrespective of the measurement error as well as noise. In the Case 2, the performance of the DS method is degraded due to the RSZ problem. In this case, the results of the DS and ILS methods may be out of the test area. The simulation results are summarized in Table 2.

Table 2: Summary of Simulation 2 (1000 Samples).

| Test Loc. | Localization Methods | | | |
|---|---------------------------------------|-------|-------|-------|
| | DS | ILS | DSRM | CKF |
| | Mean Value of the Location Errors [m] | | | |
| Standard Deviation of the Location Errors [m] | | | | |
| 2, 2 | 0.771 | 0.814 | 0.586 | 0.463 |
| | 0.436 | 0.510 | 0.358 | 0.069 |
| 5, 2.5 | 1.451 | 0.858 | 0.636 | 0.527 |
| | 0.597 | 0.498 | 0.417 | 0.189 |

4 CONCLUSIONS

In this paper, several wireless localization methods using the ranging measurements are reviewed when the measurements include non-Gaussian errors as well as Gaussian noise. The measurement errors are considered as always positive. The localization methods analysed in this paper are ILS, DS, and DSRM methods for model-free methods, and CKF for model-based Kalman filtering. First, the characteristics of each method are analysed based on the expansion of the localization equations. Then, some simulations are carried out to verify the performance of the localization methods under the measurement error occurrence. The simulation results show that the relative location errors of the DSRM method compared with the DS and ILS methods are 41.8% and 85.8%, respectively. Also, the relative location errors of the CKF compared with the DS, ILS and DSRM methods are 28.2%, 57.9% and 67.5%, respectively. Consequently, it can be concluded that the DSRM method can yield

comparatively more accurate location solution among the model-free localization methods when the ranging measurements contain non-Gaussian errors with positive numbers. In addition, the model-based Kalman filtering can enhance the localization performance compared with the model-free methods.

ACKNOWLEDGEMENTS

This research was supported by Basic Science Research Program through the National Research Foundation of Korea (NRF) funded by the Ministry of Education (NRF-2015R1D1A1A01059606).

REFERENCES

- Arasaratnam, I., Kaykin, S., 2009, Cubature Kalman filters, *IEEE Trans. Automatic Control*, vol. 54, pp. 1254-1269.
- Banani, S. A., Najibi, M., Vaughan, R. G., 2013, Range-based localization and tracking in non-line-of-sight wireless channels with Gaussian scatterer distribution model, *IET Communications*, vol. 7, pp. 2034-2043.
- Biton, I., Koifman, M., Bar-Itzhack, I. Y., 1998, Improved direct solution of the global positioning system equation, *Journal of Guidance Control and Dynamics*, vol. 21, pp. 45-49.
- Cho, S. Y., 2014, Implementation technology for localising a group of mobile nodes in a mobile wireless sensor network, *Journal of Navigation*, vol. 67, pp. 1089-1108.
- Cho, S. Y., Kang, D., Kim, J., Lee, Y. J., Moon, K. Y., 2017, Performance analysis of the wireless localization algorithms using the IR-UWB nodes with non-calibration errors, *Journal of Positioning, Navigation, and Timing*, vol. 6, no. 3, pp. 105-116.
- Cho, S. Y., Kim, B. D., 2013, Linear closed-form solution for wireless localisation with ultra-wideband/chirp spread spectrum signals based on difference of squared range measurements, *IET-Wireless Sensor Systems*, vol. 3, pp. 255-265.
- Jia, B., Xin, M., Cheng, Y., 2013, High-degree cubature Kalman filter, *Automatica*, vol. 49, pp. 510-518.
- Kolodziej, K. W., Hjelm, J., 2006, *Local Positioning Systems: LBS Applications and Services*, Taylor & Francis Group.
- Lee, B. H., Hur, H., Ahn, H. S., 2013, Environmental-adaptive bias calibration in wireless localization, *IEEE Communications Letters*, vol. 17, no. 4, pp. 717-720.
- Lee, J. Y., Scholtz, R. A., 2002, Ranging in ad dense multipath environment using an UWB radio link, *IEEE Journal of Selected Areas in Communications*, vol. 20, no. 9, pp. 1677-1683.
- Mendel, J. M., 1995, *Lessons in estimation theory for signal processing, communications, and control*, New Jersey: Prentice Hall.
- Oh, M. K., Park, J. H., Kim, J. Y., 2009, IR-UWB packet-based precise ranging system for u-home networks, *IEEE Trans. Consumer Electronics*, vol. 55, no. 1, pp. 119-125.
- Silva, B., Hancke, G. P., 2016, IR-UWB-based non-line-of-sight identification in harsh environments: principles and challenges, *IEEE Trans. Industrial Electronics*, vol. 12, no. 3, pp. 1188-1195.
- Yan, J., Tiberius, Christan C. J. M., Janssen, J. M., Teunissen, Peter J. G., Gellusci, G., 2013, Review of range-based positioning algorithms, *IEEE Aerospace and Electronic Systems Magazine*, vol. 28, no. 8, pp. 2-27.